

# Critical Dynamics of Dimers: Implications for the Glass Transition

Dibyendu Das

*Indian Institute of Technology Bombay, Powai, India 400076*

Greg Farrell, Jane' Kondev and Bulbul Chakraborty

*Martin Fisher School of Physics, Brandeis University,*

*Mailstop 057, Waltham, Massachusetts 02454-9110, USA*

## Abstract

The Adam-Gibbs view of the glass transition relates the relaxation time to the configurational entropy, which goes continuously to zero at the so-called Kauzmann temperature. We examine this scenario in the context of a dimer model with an entropy vanishing phase transition, and stochastic loop dynamics. We propose a coarse-grained master equation for the order parameter dynamics which is used to compute the time-dependent autocorrelation function and the associated relaxation time. Using a combination of exact results, scaling arguments and numerical diagonalizations of the master equation, we find non-exponential relaxation and a Vogel-Fulcher divergence of the relaxation time in the vicinity of the phase transition. Since in the dimer model the entropy stays finite all the way to the phase transition point, and then jumps discontinuously to zero, we demonstrate a clear departure from the Adam-Gibbs scenario. Dimer coverings are the “inherent structures” of the canonical frustrated system, the triangular Ising antiferromagnet. Therefore, our results provide a new scenario for the glass transition in supercooled liquids in terms of inherent structure dynamics.

PACS numbers:

## INTRODUCTION

A variety of systems such as supercooled liquids, colloids, granular matter and foams, exhibit a transition from a flowing fluid phase to a frozen solid phase. Jamming due to spatial constraints imposed on the elementary constituents of these materials has been proposed as a possible common cause of this dynamical arrest [1, 2, 3].

Model systems, such as hard spheres, have an important role to play in the investigation of such a scenario since they allow for a precise definition of jamming [4]. They are also useful in elucidating the precise relationship between thermodynamics and dynamics in materials exhibiting a jammed phase [5]. The entropy-based Adam-Gibbs theory[6] relates the viscosity (a dynamical quantity) to the configurational entropy ( $S_{conf}$ )(a thermodynamic quantity) through  $\eta = \eta_0 \exp(A/TS_{conf})$ . The ideal glass transition is associated with the Kauzmann temperature at which the configurational entropy vanishes[7]. In this paper, we explore the connection between dynamics and thermodynamics in a lattice model of dimers with an entropy-vanishing phase transition.

The dimer model is one of the working horses of statistical mechanics. It provides an example of a jammed system which has the added advantage of being exactly solvable [8]. States of the dimer model are specified by placing dimers on the bonds of the lattice so that every lattice site is covered by exactly one dimer; see Fig 1. These dimer coverings are “locally jammed” [4] as every dimer cannot move to an empty, neighboring bond, without violating the packing constraint. Moves that involve *loops* of dimers and adjacent empty bonds, on the other hand, are allowed. An example of such a move for the hexagonal lattice involving an elementary plaquette is shown in Fig. 1a. Stochastic dynamics of the dimer model on the square lattice based on these elementary moves were considered by Henley [9].

Most states of the dimer model allow for elementary moves; an example of one which does not is shown in Fig. 1b. The smallest move in this case involves a system spanning loop, and we call this state “maximally jammed”. If we define an energy functional on the space of dimer coverings which favors the maximally jammed state, a transition into this state can be affected as the temperature is lowered. The central question we address in this paper is: *What happens to relaxation time scales of the dimer model as the transition to the maximally jammed state is approached?* We will show that the relaxation is dominated by entropy barriers and is sensitive to equilibrium fluctuations near the phase transition point.

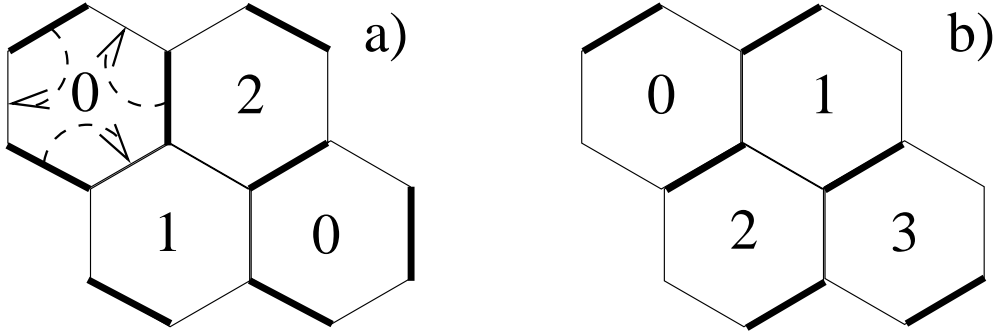


FIG. 1: (a) Dimer covering of the honeycomb lattice with an elementary loop update indicated by the arrows. The numbers are the heights of the equivalent interface. (b) An ordered, maximally jammed dimer covering; the equivalent interface is tilted with maximum slope.

We consider an energy functional that exhibits a continuous transition to the maximally jammed state along a metastable line. We find a strong departure from the canonical critical-slowing-down scenario [10], which we attribute to the presence of entropy barriers. Barriers can be traced directly to the non-local nature of the dynamical moves allowed by the jammed states. The longest relaxation time-scale is found to diverge exponentially following a Vogel-Fulcher-like form. This is reminiscent of what is observed in fragile glass formers [11]. Exponential time-scale divergence (activated scaling) is associated with critical points in models with quenched disorder[12] and it has been argued that real glasses belong to the universality class of random Hamiltonians with such exponential divergences[13]. The current model provides an explicit example of a model without quenched disorder which exhibits activated scaling. It should be mentioned that the Vogel-Fulcher law has been observed in models with entropic barriers [14], with traps [15], and within effective medium theory [16], none of which have an explicit critical point.

## DIMER MODEL

We consider the dimer model on the 2-d hexagonal lattice of linear size  $L$ , having  $2L^2$  sites and  $3L^2$  bonds, with periodic boundary conditions [17]. A useful representation of the dimer model is given by the height map which associates a discrete interface  $h(x, y)$  with every dimer covering [18]. The heights of the interface are defined on the vertices of the dual triangular lattice. The height difference  $\Delta$  between two nearest neighboring sites is  $-2$  or  $+1$

depending on whether the bond of the honeycomb lattice that separates them is occupied by a dimer or not; see Fig. 1a. Directions in which the height change is  $+\Delta$  are specified by orienting all the up pointing triangles of the dual lattice clockwise.

The dimer model has an extensive entropy. The ensemble of equal weighted dimer coverings maps to a rough surface with a gradient-square free energy [18]. Fluctuations of the surface are entropic in origin. A phase transition can be induced in the dimer model by including an energy functional which is minimized by a dimer covering corresponding to a smooth, *maximally tilted* surface which corresponds to the maximally jammed state shown in Fig. 1b.

For periodic boundary conditions the tilt vector,  $(\Delta_x h, \Delta_y h)$ , where  $\Delta_{x,y} h$  is the average height difference in the  $x$  or  $y$  direction, has only one independent component  $\rho$  [19]. In terms of  $\rho$ , the energy functional we consider can be written as:

$$\beta E(\rho) = -\frac{\mu L^2}{3}(1 + 8\rho^2), \quad (1)$$

where  $\mu$  is a dimensionless coupling, proportional to inverse temperature ( $\beta = 1/kT$ ), that drives the transition.

The entropy of the dimer model as a function of  $\rho$  was calculated exactly [17, 20]:

$$S(\rho) = L^2 \left\{ \frac{2 \ln 2}{3}(1 - \rho) + \frac{2}{\pi} \int_0^{\frac{\pi}{3}(1-\rho)} dx \ln[\cos x] \right\} \quad (2)$$

This function has a maximum at  $\rho = 0$  which is the equilibrium value at  $\mu = 0$ . For finite  $\mu$  this dimer model was previously considered in Ref. [21]. A dimer model with a similar phase transition but with an energy functional linear in  $\rho$  was solved exactly by Kasteleyn [17].

In the dimer model with the free energy  $\beta F = \beta E - S$ , and the energy and entropy given by Eqs. 1 and 2, there is an interesting phase transition along the metastable line, when the order parameter is confined to the free energy well around the zero-tilt state. Namely, at  $\mu_* = \pi/(8\sqrt{3})$ , the end-point of the metastable line, the order parameter  $\rho$  has a discontinuous jump from 0 to 1, characteristic of a first-order transition. At the same time, as  $\mu_*$  is approached from below, fluctuations of  $\rho$  around 0 diverge, as would be expected at a critical point. This transition was discussed in detail in Ref. [21]. In this paper we investigate the dynamics of the dimer model near this phase transition point.

## COARSE-GRAINED DYNAMICS

As mentioned in the introduction, the hard constraint of no overlapping of dimers, gives rise to nonlocal dynamics. We consider stochastic, Monte-Carlo dynamics based on loop updates with loops of arbitrary size; a concrete implementation is given in Ref. [22]. Since we take periodic boundary conditions, loops with different winding numbers can be formed. We restrict loop updates to loops with winding numbers  $(0, 0)$ ,  $(1, 0)$  and  $(0, 1)$ , only. The microscopic transition rates for loop updates are given by Metropolis rules that follow from the energy function, Eq. 1.

Given the microscopic loop dynamics, which satisfy conditions of ergodicity and detailed balance, we ask what are the coarse-grained dynamics of the order parameter,  $\rho$ . Since the energy function in Eq. 1 depend on the global tilt  $\rho$  only, it follows that all updates of topologically trivial loops (i.e. those with  $(0, 0)$  winding number) have  $\Delta E = 0$ . Only when system spanning loops with nonzero winding numbers are updated does the energy of the state change. This feature naturally leads to fast and slow processes in the Monte-Carlo dynamics. On a faster time scale, non-winding loops are updated with no effect on the overall tilt of the surface, while on a much slower time scale, winding loops are updated causing a change in the tilt of the surface.

The *coarse-grained* dynamics of global tilt changes are described by a master equation for the probability ( $P_\rho$ ), that the dimer model has tilt  $\rho$ ,

$$\frac{dP_\rho}{dt} = - \left[ W_{\rho-1/L, \rho} + W_{\rho+1/L, \rho} \right] P_\rho + W_{\rho, \rho-1/L} P_{\rho-1/L} + W_{\rho, \rho+1/L} P_{\rho+1/L} . \quad (3)$$

The rates in this master equation obey the detailed balance condition:  $W_{\rho-1/L, \rho} / W_{\rho, \rho-1/L} = \exp[-(F(\rho - 1/L) - F(\rho))]$ . The usual way of achieving this balance which leads to normal diffusive dynamics is to partition the rates symmetrically with  $W_{\rho-1/L, \rho} \simeq \exp[-(F(\rho - 1/L) - F(\rho))/2]$  and  $W_{\rho, \rho-1/L} = \exp[(F(\rho - 1/L) - F(\rho))/2]$ [23]. Equation 3, however, features an unusual form for the transition rates between different tilt states. Namely, the rates of transitions from higher into lower tilt states (increasing energy transitions) are determined by the energy change alone:

$$W_{\rho-1/L, \rho} = \Gamma_0 e^{-(E(\rho-1/L) - E(\rho))} ; \quad (4)$$

here  $\Gamma_0$  is a constant. This follows from the observation that in order to lower the tilt and increase the energy, a system spanning loop, which is always present in a state with  $\rho \neq 0$ ,

needs to be updated. This form of the rates for energy-increasing transitions in conjunction with the detailed balance condition implies that the rates of transitions to higher tilt states (energy lowering transitions) must be determined by the entropy change:

$$W_{\rho, \rho-1/L} = \Gamma_0 e^{-(S(\rho-1/L)-S(\rho))} . \quad (5)$$

The form of the transition rates that we are arguing for here, was directly observed in numerical simulations of the three coloring model [24], which is a close relative of the dimer model. The two are equivalent if, in the dimer models, a weight of 2 is attached to each loop formed by bonds that are not covered by dimers.

## RELAXATION TIME-SCALES

The first consequence of the above form of the transition rates is that the time scale of relaxation out of a state with tilt  $\rho$ ,  $\tau_\rho = 1/(W_{\rho-1/L, \rho} + W_{\rho+1/L, \rho})$ , is a *non-decreasing* function of  $\rho$ . The exact expressions for  $\tau_\rho$  (measured in units of  $\Gamma_0^{-1}$ ),

$$\tau_\rho^{-1} = e^{-\frac{16}{3}\rho\mu L} + e^{-L[\frac{2}{3}\ln 2 + \frac{2}{3}\ln[\cos(\frac{\pi}{3} - \frac{\pi\rho}{3})]]}, \quad (6)$$

follows from Eqs. 4 and 5, and it is plotted in Fig. 2a). This time-scale increases monotonically with  $\rho$ [25], as in the hierarchical models of Palmer *et al.* [26]. It is in sharp contrast with canonical Langevin dynamics around the equilibrium state, for which the time to relax out of a macro-state *decreases* the further the order parameter is away from its equilibrium value. (For example, in the Ising model with Glauber dynamics and in the disordered phase, the relaxation time out of a given magnetization state *decreases* with increasing magnetization.)

## AUTOCORRELATION FUNCTION

To quantify the tilt dynamics we compute the tilt-tilt autocorrelation function  $C(t)$ , defined as:

$$C(t) = \frac{\langle \rho(t)\rho(0) \rangle - \langle \rho(0) \rangle^2}{\langle \rho(0)^2 \rangle - \langle \rho(0) \rangle^2}, \quad (7)$$

with the average taken over different histories of  $\rho$ . An approximate form for the autocorrelation function is:

$$C(t) \approx \frac{\sum_\rho (\rho - \langle \rho \rangle)^2 e^{-F(\rho)} e^{-t/\tau_\rho}}{\sum_\rho (\rho - \langle \rho \rangle)^2 e^{-F(\rho)}}, \quad (8)$$

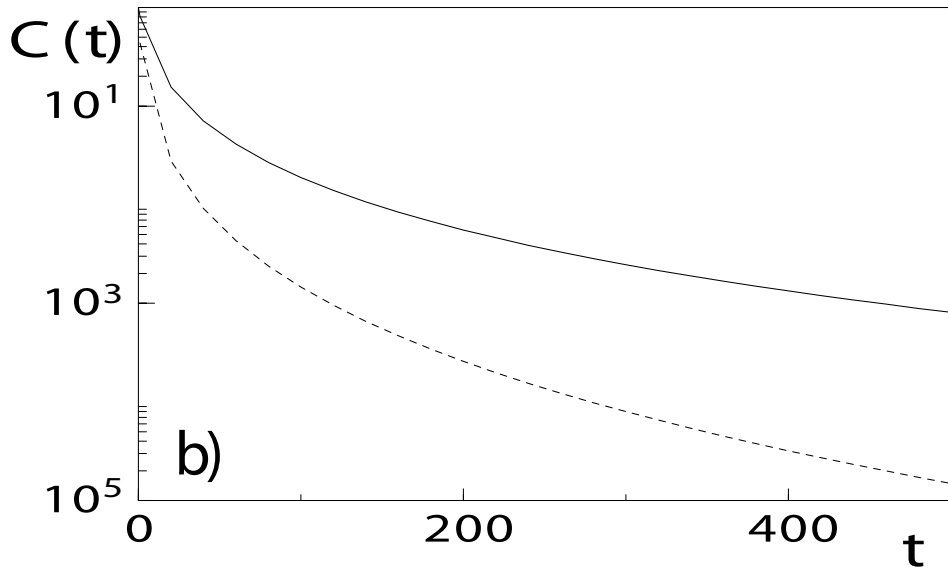
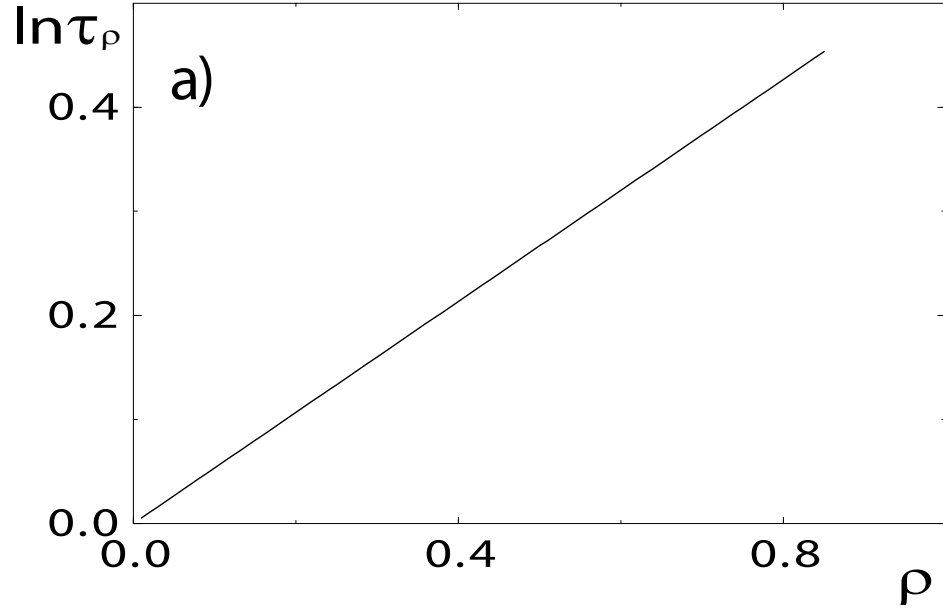


FIG. 2: (a) The time scales for relaxing out of different tilt states  $\rho$  in the dimer model (scaled by  $L$ ), for a value of  $\mu$  below the transition. (b) The tilt-tilt autocorrelation function of the dimer model. The full line is obtained from Eq. 8 while the dashed line is a result of the saddle point evaluation of Eq. 8. Here  $L = 4096$  and time is measured in units of  $\Gamma_0^{-1}$ .

i.e.,  $C(t)$  is an equilibrium weighted average of relaxations out of different  $\rho$  states. This approximation is based on the assumption that eigenfunctions of the rate matrix are localized in  $\rho$ -space and eigenfunctions corresponding to different eigenvalues do not have significant overlaps. We will justify this assumption *a posteriori* by examining the eigenfunctions obtained from numerical diagonalizations of the rate matrix  $W_{\rho,\rho'}$ . The asymptotic decay of the autocorrelation functions can be extracted by performing a saddle point analysis of the sum in Eq. 8 and using a quadratic approximation for the entropy (Eq. 2). These saddle point solution is compared in Fig. 2b) to the result obtained from the sum (Eq. 8).

In the limit of  $\mu \rightarrow \mu_*$  and  $t \rightarrow \infty$ , saddle point analysis yields:

$$C(t) \sim \exp\left\{-\frac{3}{32}\left(\frac{\mu_* - \mu}{\mu_*^2}\right)\left[\ln\left(\frac{2\mu_* t}{\mu_* - \mu}\right)\right]^2\right\}, \quad (9)$$

showing that  $C(t)$  in the dimer model has a log-normal form implying a slower than exponential decay. From Eq. 9 we also conclude that the relaxation timescale,  $\tau$ , for the decay of  $C(t)$  to an arbitrary constant  $C_0$ , diverges exponentially as  $\mu \rightarrow \mu_*$ . This is a Vogel-Fulcher type behavior (since  $\mu$  is proportional to  $\beta = 1/kT$ ) observed in many fragile glass formers. First order corrections to Eq. 9 lead to an even more rapid increase of time scales, with  $\tau/\ln\tau$  diverging as Vogel-Fulcher.

The coarse grained dynamics defined by the transition matrix elements, Eqs. 4 and 5, were argued to follow from the nonlocal loop dynamics of the dimer models. From this form of the  $W$ -matrix all the conclusions about critical dynamics of the dimer model are derived. We have confirmed this picture in considerable detail in simulations of the three coloring model [27, 28], which, as discussed earlier, is the loop weighted dimer model. The loop weights are not expected to affect the qualitative features of the energy and entropy functionals. Indeed, the measured  $\tau_\rho$  for the three-coloring model compare very well [27, 28] to the analytical form plotted in Fig. 2. The numerical evidence for Vogel-Fulcher type divergence of the relaxation time scale in this model was reported previously [27].

The dynamical behavior of the dimer model can be traced back to the interplay between the free energy and dynamical barriers. The transition rates presented in Eqs. 4 and 5, can be interpreted in terms of a barrier[26]  $B(\rho) = e^{(S(\rho-1/L)-S(\rho)+(E(\rho-1/L)-E(\rho)))/2}$  dividing the usual Metropolis rates defined in terms of the free energy:

$$W_{\rho-1/L,\rho} = \Gamma_0 e^{-(F(\rho-1/L)-F(\rho))/2} / B(\rho) \quad (10)$$



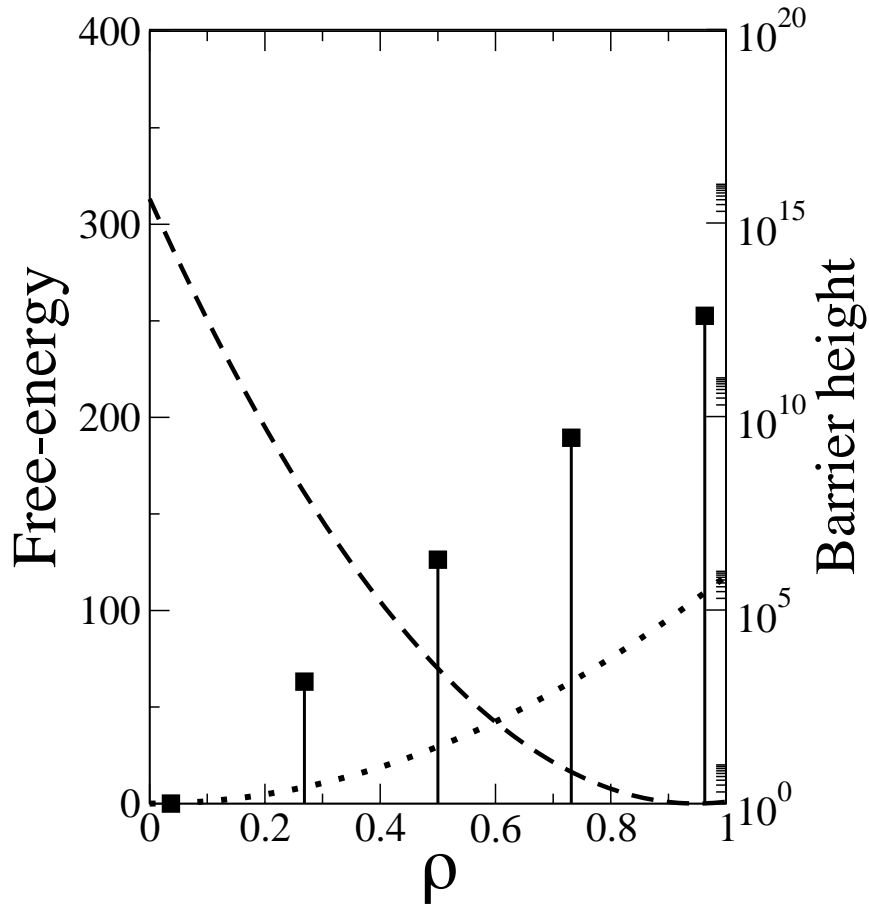


FIG. 3: Barrier height,  $B(\rho)$  (dimensionless) shown as a set of solid lines, and the quadratic approximation to the dimensionless free energies of the dimer model (dashed line);  $\mu$  is chosen close to  $\mu_*$  and  $L = 24$ . Note the logarithmic scale for the barrier height.

and

$$W_{\rho, \rho-1/L} = \Gamma_0 e^{(F(\rho-1/L) - F(\rho))/2} / B(\rho) \quad (11)$$

The barriers increase exponentially with  $\rho$  as illustrated in Fig. 3. Dynamics of the order parameter can be viewed as relaxation in the free energy well in the presence of these barriers.

## SCALING ANALYSIS OF THE MASTER EQUATION

The emergence of the Vogel-Fulcher law in the dimer model, based on the master equation with transition rates defined in Eqs. 10 and 11, follows from a scaling argument.

At the critical point,  $\mu = \mu^*$ , the free energy difference between different tilt states close to  $\rho = 0$  vanishes. In this limit, the transition rates are symmetric and given by:

$$W_{\rho-1/L,\rho} = W_{\rho,\rho-1/L} = \Gamma_0/B(\rho). \quad (12)$$

The diffusion constant in this symmetric case can be shown to be given by [29, 30]:

$$D(L) = L\Gamma_0/(\sum_{i=-L,L} B(\rho_i)) \quad (13)$$

where  $L$  is the system size and  $\rho_i = i/L$ . The longest timescale in the problem is given by

$$\tau(L) = L^2/D(L) \quad (14)$$

In the limit of large  $L$ , the summation in Eq. 13 can be replaced by an integral. If we make use of the quadratic approximation to the entropy (Eq. 2) then  $B(\rho) = e^{(8/3)(\mu+\mu^*)L\rho}$  and the integral can be evaluated analytically, with the result:

$$\tau(L) = \frac{L}{\Gamma_0} \left( e^{\frac{16}{3}\mu^*L} - 1 \right) \quad (15)$$

Note that the same result can be obtained by replacing the summation by the largest barrier which occurs at  $\rho = 1$ . The longest time-scale in the system is, therefore, seen to diverge *exponentially* with system size. If all the barriers were equal to one, then we would have  $D(L) = \Gamma_0$  and  $\tau(L) = L^2/\Gamma_0$ , which corresponds to simple diffusion. In the presence of the barriers,  $D(L)$  goes to zero exponentially and this leads to an exponential divergence of the relaxation time-scale.

We can now use a scaling argument to deduce the behavior of the relaxation time-scale for  $\mu < \mu^*$ . The effective scale (in  $\rho$ -space) over which the free-energy well is flat, and therefore the transition rates are symmetric, diverges as the phase transition at  $\mu = \mu^*$  is approached. We argue that this length scale, given by  $l(\mu) = \frac{\sqrt{\mu^*}}{\sqrt{\mu^*-\mu}}$ , provides a cutoff to the summation (or integral) involved in calculating the diffusion constant

$$D(l) = \Gamma_0 l / (\sum_{i=-l(\mu),l(\mu)} B(\rho_i)) \quad (16)$$

The longest time scale therefore scales as

$$\tau(\mu) = \tau(l(\mu)); \quad l(\mu) < L \quad (17)$$

and

$$\tau(\mu) = \tau(L); \quad l(\mu) \geq L . \quad (18)$$

In the thermodynamic limit,  $\tau(\mu)$  diverges as  $\tau(\mu) \simeq e^{(16/3)\frac{\sqrt{\mu_*}}{\sqrt{\mu_*-\mu}}}$ . Since  $\mu \simeq 1/T$ ,  $\tau$  has a Vogel-Fulcher type divergence  $\tau(T) \simeq e^{(16/3)\frac{\sqrt{T_*}}{\sqrt{T-T_*}}}$ .

We have recently shown that the Vogel-Fulcher divergence of the dimer model can be obtained from an exact solution of the continuum version of the master equation if we assume that  $S(\rho)$  has a quadratic form [31].

## NUMERICAL ANALYSIS OF THE MASTER EQUATION

We have carried out numerical diagonalizations of the rate matrix for  $L \times L$  systems in order to verify some of the assumptions that have been made in the scaling analysis and in the calculation of the correlation function. These computations also provide us with information about the finite-size effects on the critical dynamics of the dimer model.

The probability distribution,  $P(\rho, t)$ , can be written in terms of the eigenvalues,  $\lambda_i$ , and eigenfunctions,  $\psi_i(\rho)$  of the rate matrix[23]:

$$P(\rho, t) = \sum_i \psi_i(\rho) e^{-\lambda_i t} \quad (19)$$

The eigenvalues of the rate matrix are non-negative and the equilibrium distribution is given by the zero-eigenvalue function,  $\psi_1$  ( $\lambda_1 = 0$ ). The smallest, non-zero eigenvalue characterizes the state with the longest relaxation time. All correlation functions can be expressed in terms of the eigenvalue spectrum and, in particular, the equilibrium, tilt-tilt autocorrelation function can be written as:

$$C(t) = \sum_i e^{-\lambda_i t} \sum_{\rho\rho'} \rho\rho' e^{-(F_\rho+F_{\rho'})/2} \psi_i(\rho) \psi_i^*(\rho') \quad (20)$$

Comparing to Eq. 8 it follows that the approximate form is obtained in the limit of delta-function localized eigenfunctions. We will show below that the eigenfunctions corresponding to non-zero eigenvalues of the dimer model are indeed well localized.

Results of the numerical diagonalization, using the exact entropy function, show that the longest time scale,  $\tau$ , of the dimer model increases in a non-arrhenius, Vogel-Fulcher fashion, as shown in Fig. 4. The scaling in this figure is what is expected from the scaling solution of the model with the quadratic entropy [31] and similar to the results obtained from the scaling arguments presented in this paper, however the length scale emerging is  $l(\mu) = [\frac{\mu^*}{\mu^* - \mu}]^2$  not  $l(\mu) = \frac{\sqrt{\mu^*}}{\sqrt{\mu^* - \mu}}$ , as would be expected from the quadratic entropy results [31].

The exact diagonalization results show, unambiguously, that the Vogel-Fulcher law characterizes the time scale divergence at the entropy vanishing transition in the dimer model.

### Eigenfunctions

In the dimer model, the eigenfunction corresponding to the smallest non-zero eigenvalue is localized at the largest barrier, i.e, the largest value of  $\rho$ . Higher eigenfunction move to smaller barriers but are still localized. The expression we used for  $C(t)$  is exact for delta-function localization of eigenfunctions and the numerical results justify this assumption, *a posteriori*.

### Sensitivity of dynamics to barrier size

The sensitivity of the relaxation times to the barriers heights has been investigated by using the quadratic entropy model and writing  $B(\rho) = e^{\frac{c}{2}(S(\rho - 1/L) - S(\rho) + (E(\rho - 1/L) - E(\rho)))/2}$  and varying  $c$  between 0 and 1. For  $c = 0$ , we recover the usual Langevin dynamics and the time scales should increase as a power law and for  $c = 1$  we have barriers corresponding to the loop dynamics. The results plotted in Fig 6 demonstrate that, for  $c = 0$ ,  $\tau \simeq (\mu^* - \mu)^{-1}$  which is consistent with a dynamical exponent  $z = 2$  and a correlation length exponent of  $\nu = 1/2$ ; the exponents expected from a Langevin description of a mean-field model. It is also clearly seen from this figure that even for  $c = 0.25$ , the timescale increases more rapidly than a power law. An analysis of the continuum limit of the dimer model dynamics shows that, for any non-zero value of  $c$ ,  $\tau \simeq e^{A(c^{2l(\mu)})}$  where  $A$  is a constant [31, 32]. These results taken all together imply that there is a whole class of systems, where dynamical constraints may lead to

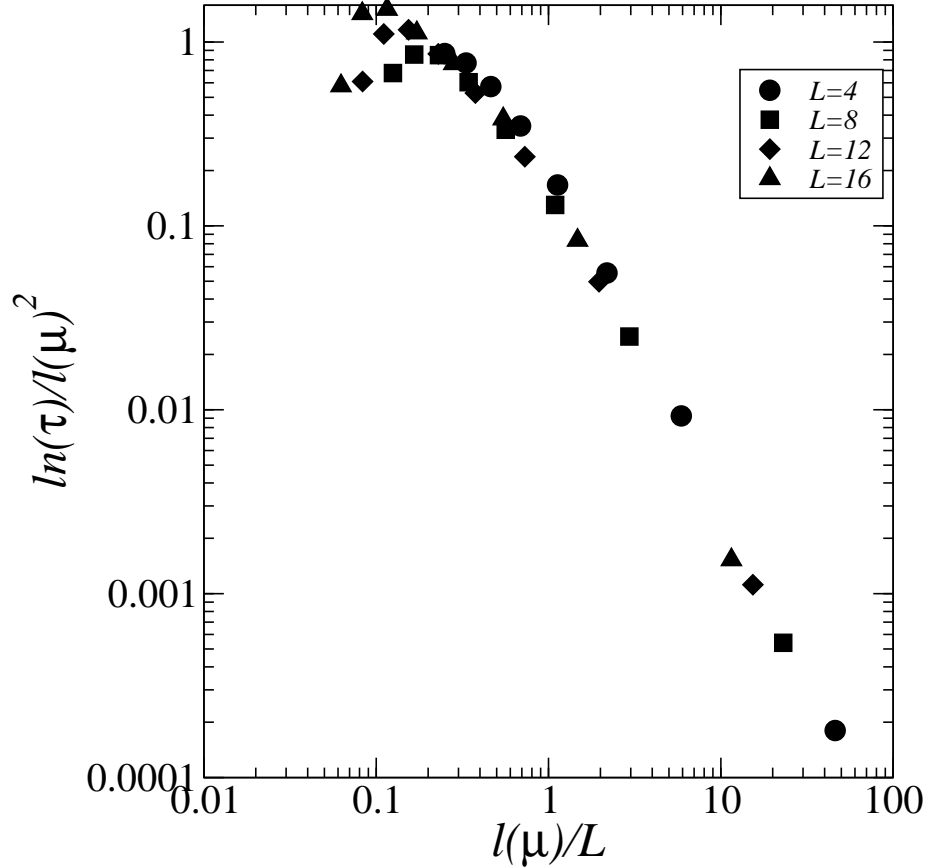


FIG. 4: Scaling of  $\tau(\mu, L)$  in the dimer model. The figure shows that a scaling form can be constructed in terms of the lengthscale  $l(\mu) = (\mu^*/(\mu^* - \mu))^2$  and the particular form demonstrates the Vogel-Fulcher scaling  $\tau \simeq e^{(l(\mu))^2}$ .

non-zero values of  $c$ , which belong to different universality classes of dynamical critical phenomena. These are characterized by a Vogel-Fulcher rather than a power-law divergence of relaxation time-scales, with  $c$  being an indicator of fragility [11]. In real systems, such as supercooled liquids, one expects that there is a large but finite energy scale at which

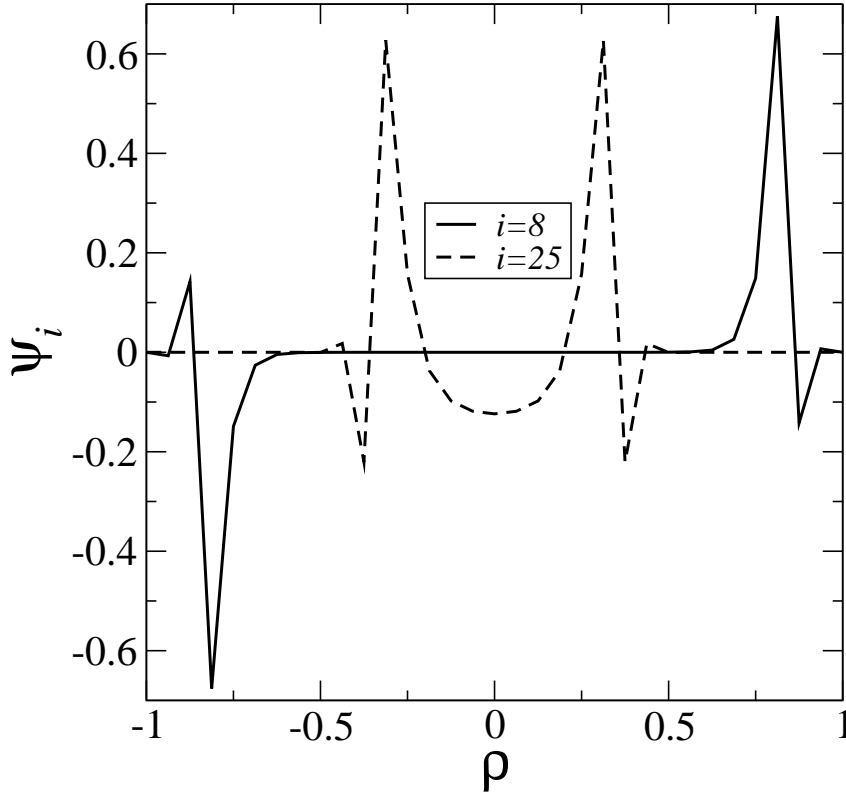


FIG. 5: Plots of the eighth and twenty-fifth eigenfunctions of the dimer model for  $L=16$  and  $\mu \simeq \mu^*$ . These two eigenfunctions were chosen to illustrate the localization of the eigenfunctions and the shift towards  $\rho = 0$  with increasing spectral index

the hard constraints are violated. This energy scale then leads to a long-time cutoff of the Vogel-Fulcher behavior. This time scale, may however, be well beyond any experimentally measurable time scales.

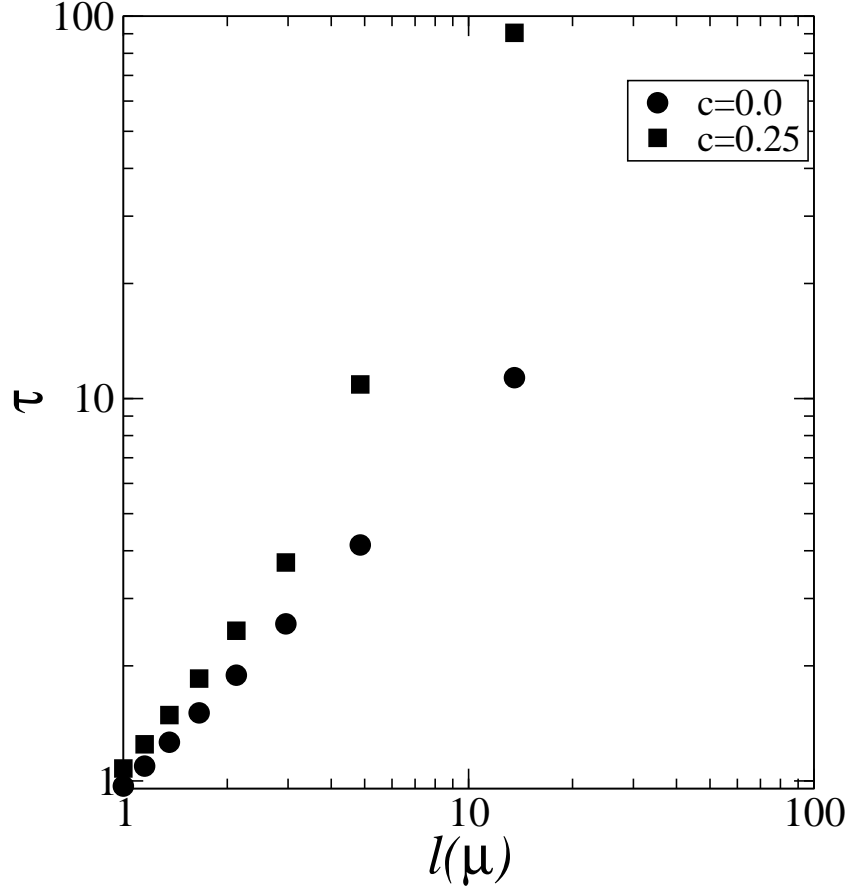


FIG. 6: Timescale  $\tau$  in the dimer model for different values of the barrier strength,  $c$ , plotted as a function of  $l(\mu) = \frac{\mu^*}{\mu^* - \mu}$

### ADAM-GIBBS SCENARIO

The entropy of the dimer model,  $S_{conf}$ , which corresponds to  $S(\rho)$  evaluated at the equilibrium value of the order parameter  $\rho$ , goes to zero at the transition. Furthermore, our results clearly show that the longest time scale diverges in a Vogel-Fulcher manner. The

Adam-Gibbs relation,  $\tau = \tau_0 e^{A/S_{conf}(T)}$ , however, does not capture the physics since in the dimer model,  $S_{conf}$  jumps from a finite value at  $\rho = 0$  to zero, as  $\rho$  changes discontinuously to 1. Thus, in this model, the exponential divergence of the relaxation time-scale at the transition is not accompanied by a continuous vanishing of  $S_{conf}$ . The analysis presented in this paper clearly demonstrates that the Vogel-Fulcher divergence is rooted in the constraints which lead to loop dynamics. This type of nonlocal dynamics leads to the unusual transition rates with energy-lowering transitions being determined by changes in entropy and, therefore, to an exponential decrease of the number of energy-lowering trajectories as one approaches the zero-entropy state.

The configurational entropy of supercooled liquids has been interpreted as the inherent structure entropy, i.e., the number of valleys at the temperature of interest. The observation that the Adam-Gibbs scenario describes much of the phenomenology of supercooled liquids could imply that there is a phase transition in the inherent-structure space similar to the one discussed in this paper for dimers. Experiments and simulations have shown that a hallmark of supercooled liquids approaching the glass transition is the appearance of dynamical heterogeneities[3, 33, 34]. The loops in the dimer dynamics are analogs of these dynamical heterogeneities since they define the correlated moves allowed by the constraints. These heterogeneities are present as long as the constraints are not violated and are characterized by a size distribution which changes as the critical point is approached[27, 28]. The analogy between loops and dynamical heterogeneities suggest that the dynamics in the inherent structure space of supercooled liquids could be similar to the loop dynamics of dimer models. If this is the case then transition rates between inherent structures should exhibit features similar to the ones discussed in this paper. We are currently in the process of analyzing transition rates between inherent structures of Lennard-Jones glass formers in order to get a better understanding of the connection between dynamical heterogeneities and the effective dynamics in the inherent-structure space.

The authors would like to acknowledge numerous useful discussions with Satya Majumdar. This work was supported by grants from the NSF: DMR-0207106 (DD and BC), DMR-9984471 (JK) and DMR-0403997 (BC and JK). JK is a Cottrell Scholar of Research Corporation.



- 
- [1] S. F. Edwards and D. V. Grinev, in *Jamming and Rheology: Constrained Dynamics on Microscopic and Macroscopic Scales*, eds A. J. Liu and S. R. Nagel, (Taylor and Francis, New York, 2001).
- [2] C.S. O’Hearn, S.A. Langer, A.J. Liu and S.R. Nagel, *Phys. Rev. Lett.* **2001**, 86, 111 .
- [3] V. Trappe *et al.*, *Nature* **2001**, 411, 772.
- [4] S. Torquato and F.H. Stillinger, *J. Phys. Chem. B* **2001**, 105, 11849.
- [5] L. Santen and W. Krauth, *Nature* **2000**, 405, 550.
- [6] G. Adam, J. H. Gibbs, *J. Chem. Phys.*, **1965**, 43, 139.
- [7] L.-M. Martinez, C. A. Angell, *Nature* **2001**, 410, 663.
- [8] J.F. Nagle, C.S.O. Yokoi, and S.M. Bhattacharjee, in *Phase transitions and Critical Phenomena*, eds C. Domb and J.L. Lebowitz, Vol. 13, p. 235 (Academic Press, 1989).
- [9] C.L. Henley, *J. Stat. Phys.* **1997**, 89, 483.
- [10] P.C. Hohenberg and B.I. Halperin, *Rev. Mod. Phys.* **1977**, 49, 435.
- [11] C.A. Angell, *J. Phys. Chem.* **1988**, 49, 863.
- [12] D. S. Fisher, *Phys. Rev. Lett.* **1986**, 56, 416.
- [13] G. Parisi, cond-mat/9411115
- [14] F. Ritort, *Phys. Rev. Lett.* **1995**, 75, 1190; C. Godrèche, J.P. Bouchaud and M. Mézard, *J. Phys. A: Math. Gen.* **1995**, 28, L603-L611.
- [15] C. Monthus and J-P. Bouchaud, *J.Phys. A* **1996**, 29, 3847.
- [16] N. Kumar, cond-mat pre-print/ 0407688.
- [17] P.W. Kasteleyn, *J. Math. Phys.* **1963**, 4, 287.
- [18] H.W.J. Blöte and H.J. Hilhorst, *J.Phys. A* **1982**, 15, L631.
- [19] The components of the tilt along the three lattice directions of the triangular lattice are subject to two constraints. One arising from the conservation of the total dimer number ( $= L^2$ ) and the other from periodic boundary conditions which force two of the components to be equal.
- [20] A. Dhar, P. Chaudhuri and C. Dasgupta, *Phys. Rev. B* **2000**, 61, 6227.
- [21] H. Yin and B. Chakraborty, *Phys. Rev. Lett.* **2001**, 86, 2058, and *Phys. Rev. E* **2002**, 65, 036119.
- [22] W. Krauth and R. Moessner, *Phys. Rev. B* **2003**, 67, 064503.

- [23] L. E. Reichl, *A modern Course in Statistical Physics*, (Wiley Interscience, NY), 1998.
- [24] D. Das, J. Kondev, and B. Chakraborty, *Europhys. Lett.* **2003**, 61, 506.
- [25] Since the phase transition occurs along the metastable branch in the dimer model, the range of  $\rho$ 's participating in the dynamics is restricted to  $\rho \leq \rho_{max}$ . The free energy has a maximum at  $\rho_{max}$  which vanishes as  $\mu \rightarrow \mu_*$  and scales with the system size.
- [26] R.G. Palmer, D.L. Stein, E. Abrahams and P.W. Anderson, *Phys. Rev. Lett.* **1984**, 53, 958; S. Teitel, *Phys. Rev. Lett.* **1988**, 60, 1154.
- [27] B. Chakraborty, D. Das and J. Kondev, *Eur. Phys. J. E.* **2002**, 9, 227.
- [28] B. Chakraborty, D. Das and J. Kondev, *Physica A* **2003**, 318, 23, and unpublished.
- [29] B. Derrida, *J. Stat. Phys.* **1983**, 31, 433.
- [30] R. Zwanzig, *J. Stat. Phys.* **1982**, 28, 127.
- [31] Satya Majumdar, Dibyendu Das, Jane' Kondev, Bulbul Chakraborty, *Phys. Rev. E* **2004**, 70, 060501(R).
- [32] Dibyendu Das, unpublished.
- [33] M.D. Ediger, *Annu. Rev. Phys. Chem* **2000**, 51, 99; H. Silesco, *J. Non-Cryst Solids* **1999**, 243, 81.
- [34] S. C. Glotzer, *J. Non-Cryst Solids* **2000**, 274, 342.